Differentiating Between Psychogenic Nonepileptic Seizures and Epilepsy Based on Common Spatial Pattern of Weighted EEG Resting Networks

Peng Xu*, Xiuchun Xiong, Qing Xue, Peiyang Li, Rui Zhang, Zhenyu Wang, Pedro A. Valdes-Sosa, Yuping Wang*, and Dezhong Yao*

***Abstract*—Discriminating psychogenic nonepileptic seizures (PNES) from epilepsy is challenging, and a reliable and automatic classification remains elusive. In this study, we develop an approach for discriminating between PNES and epilepsy using the common spatial pattern extracted from the brain network topology (SPN). The study reveals that 92% accuracy, 100% sensitivity, and 80% specificity were reached for the classification between PNES and focal epilepsy. The newly developed SPN of resting EEG may be a promising tool to mine implicit information that can be used to differentiate PNES from epilepsy.**

***Index Terms*—Brain network, common spatial pattern of brain network topology, psychogenic nonepileptic seizures (PNES), resting scalp EEG.**

I. Introduction

PHYCHOGENIC nonepileptic seizures (PNES) are paroxysmal episodes of altered behavior. PNES are different from conventional epileptic seizures because they lack the expected electroencephalographical epileptic changes and the association with central nervous system dysfunction [1]–[3]. PNES are commonly mistaken for epileptic seizures (ES), resulting in a diagnostic delay of 7–10 years, on average [4], [5]. The misclassification of PNES as ES imposes health and economic burdens at the individual and population levels. Misdiagnosed PNES patients are unnecessarily prescribed multiple high-dose antiepileptic medications (AEDs) with the potential for adverse effects and teratogenicity [5]–[9]. PNES is a complex disorder that remains poorly understood and poorly managed in clinical settings [1], [2], [4], [10], [11]. Early diagnosis of PNES is critical to limit inappropriate and potentially harmful treatments and to reduce unnecessary costs associated with the illness [5]–[7], [12], [13].

Previous studies have increasingly focused on identifying criteria that can differentiate PNES based on its phenomenology [3], [5], [8], [14]. By establishing phenomenological criteria for PNES in the nineteenth century, Charcot and Gowers were the first clinicians to differentiate PNES from ES [15]. Recently, semiology, such as awareness during the ictal phase, fluttering of the eyes, and the ability of bystanders to modulate the intensity of the symptoms, has been used for the initial discrimination of PNES from epilepsy [2], [5]. In a prospective study, six semiological features that can reliably differentiate PNES from epilepsy were identified [5]. Another study, which was based on video-EEG analysis and automatic clustering, reported five clinical subtypes that adequately represent the main semiological characteristics of PNES [16]. Due to the complex interaction of heterogeneous characteristics in the PNES population, computational methods have also been explored. For example, using a self-assessment questionnaire in conjunction with an artificial neural network, a sensitivity and a specificity of 85% were observed [17]. Other diagnostic techniques have been proposed, such as the Minnesota Multiphasic Personality Inventory (MMPI), physiological measures, single photon emission computed tomography (SPECT) scans, and symptoms during the ictal and postictal states [2], [7]. However, the diagnostic success in terms of sensitivity and specificity varies significantly across studies [2], [7].

The main reason that PNES cannot be sufficiently discriminated from epilepsy is that the neural mechanisms of PNES are unclear [2]–[4], [9], [14], [18], [19]. Many MRI-based studies have shown that the majority of epilepsies are associated with brain network abnormalities [20], [21]. Compared to epilepsy, few MRI related studies have been carried out for PNES. Using a broad analysis of neuroimaging studies, some researchers have suggested that PNES arises from alterations in cognitive-emotional executive control and that an imbalance between

Manuscript received July 2, 2013; revised January 27, 2014; accepted January 29, 2014. Date of publication February 7, 2014; date of current version May 15, 2014. This work was supported in part by grants from the National Nature Science Foundation of China (#61175117, #81330032, #91232725, and #31100745), the 973 Program 2011CB707803, the program for New Century Excellent Talents in University (#NCET-12-0089), the 111 Project (B12027), and the 863 Project 2012AA011601. *Asterisks indicate corresponding authors.*

*P. Xu is with the Key Laboratory for NeuroInformation of the Ministry of Education, School of Life Science and Technology, University of Electronic Science and Technology of China, Chengdu 610054, China (e-mail: xupeng@uestc.edu.cn).

X. Xiong, P. Li, R. Zhang, Z. Wang, and *D. Yao are with the Key Laboratory for NeuroInformation of the Ministry of Education, School of Life Science and Technology, University of Electronic Science and Technology of China, Chengdu 610054, China (e-mail: xiongxiuchun@163.com; heimonu@163.com; realzhang9@gmail.com; zyu44444@163.com; dyao@uestc.edu.cn).

P. A. Valdes-Sosa is with the Key Laboratory for NeuroInformation of the Ministry of Education, School of Life Science and Technology, University of Electronic Science and Technology of China, Chengdu 610054, China, and also with Cuban Neuroscience Center, Habana 6 CP 10600, Cuba (e-mail: peter_valdes@yahoo.com).

Q. Xue and *Y. Wang are with the Department of Neurology, Xuanwu Hospital, Capital Medical University, Beijing 100053, China, and also with Beijing Key Laboratory of Neuromodulation, Beijing 100053, China (e-mail: 40209629@qq.com; mdwangyp@yahoo.com.cn).

Color versions of one or more of the figures in this paper are available online at http://ieeexplore.ieee.org.

Digital Object Identifier 10.1109/TBME.2014.2305159

these functions permits the manifestation of predetermined tendencies [2], [10]. A recent study using resting-state functional MRI (fMRI) on PNES patients and healthy controls found an abnormal functional correlation between the precentral sulcus and the insula [11]. Another study by Ding using both fMRI and structural MRI (sMRI) found that PNES patients exhibited altered smallworldness in both the functional and structural networks shifted toward a more regular (lattice-like) organization [22]. These studies revealed that PNES is also correlated with the altered interactions among multiple brain areas and that the network information may be a potential marker for PNES differentiation.

The established PNES early diagnostic approaches require detailed information, such as semiology, self-assessed scores or long-recorded video-EEGs [2], [5]–[7], [13], [14], [17], [23]–[25], and the collection of this information is very time consuming. Moreover, the experience of the clinician leads to the use of different criteria to define and select the necessary information, ultimately influencing the diagnosis of PNES.

Because studies have indicated that both epilepsy and PNES are correlated with a network abnormality in the brain, it is possible to accurately diagnose PNES and epilepsy based on a network analysis. In network analysis, properties such as local information processing and global information efficiency can be quantitatively represented by statistical measurements such as clustering coefficients and the shortest path length [26]–[28]; these properties have been adopted as features for other early disease diagnosis [29]–[31]. These statistical measurements are determined by the network spatial topology; however, the complete spatial information of a network is significantly more complex than the adopted statistical measurements. Identifying the essential spatial information of a network would be meaningful for further improving the ability to differentiate between various diseases.

In the early 1990s, the use of common spatial pattern analysis (CSP) was proposed to distinguish between normal and abnormal EEGs and also to extract abnormal components from EEGs [32], [33]. In this paper, we take advantage of the fact that the weighted adjacency matrix of the brain network contains the fundamental spatial information and that CSP may identify the differentiating features in the weighted adjacency matrix. We assume that the common spatial pattern extracted from the brain network topology (SPN) may be helpful for distinguishing between PNES and epilepsy.

Because scalp EEG is relatively inexpensive and easily recorded, it is widely used for the diagnosis and classification of epilepsy [34]–[36]. In this study, we evaluate the feasibility of using resting scalp EEG to differentiate between PNES and epilepsy based on the statistical properties and SPN of EEG brain networks.

II. Methods

A. Patients and Controls

Fifteen PNES subjects were recruited from the epilepsy outpatient and inpatient departments of Xuanwu Hospital; 15 age- and sex-matched healthy subjects were recruited from advertisements posted at Capital Medical University and on the Internet from 2010 to 2012. An additional 10 subjects with focal epilepsy participated in the study. All experimental protocols were approved by the Ethics Committee of Xuanwu Hospital of Capital Medical University. Informed consent was obtained from all participants in accord with the Declaration of Helsinki. The diagnoses were conducted by two senior epileptologists with experience in diagnosing and treating epilepsy.

The PNES patients studied here satisfied the following inclusion criteria [37], [38]: 1) episode details described by witnesses lacked association with central nervous system dysfunction and were suspected by two senior epileptologists; 2) each suspected subject underwent either an inpatient or outpatient video-EEG recording for at least 12 h to record a minimum of two spontaneous or provoked nonepileptic events that were identified as nonepileptic seizures by two epileptologists. Moreover, witnesses familiar with the patient's seizures agreed that the recorded episodes were typical; 3) interictal 24-channel EEG showed no abnormal epileptic discharge based on the review of two EEG experts; 4) the ictal 24-channel EEG exhibited no abnormality based on the review of two EEG experts.

Inclusion criteria for the local epilepsy group included the following: 1) the epilepsy was identified by both MRI scanning and video-EEG; 2) interictal 24-channel EEG exhibited an abnormality based on the review of two EEG experts.

Inclusion criteria for the healthy control (HC) group included: 1) no previous history of an episode and 2) interictal 24-channel EEG showing no abnormality based on the review of two EEG experts.

B. EEG Recording and Preprocessing

Each EEG was recorded continuously at 60 sites using electrodes set in an elastic cap (Greentek, Wuhan, China), which was positioned according to the 10–10 international system, including references, ground, ECG and EOG. The reference was placed at the CPz site between Cz and Pz, and the ground electrode was placed in front of Fpz. Horizontal and vertical eye movements were detected by recording the electro-oculogram (EOG) with the use of two additional electrodes, placed 1 cm below (left side) and above (right side) the external canthus. The data were recorded with an amplifier (Micromed, Italy) using a band-pass filter of 0.5–70 Hz, a notch of 50 Hz, and a sampling rate of 512 Hz.

The electrode-skin impedance was set at less than 5 kΩ. All recordings were obtained in the morning when the subjects were resting comfortably. An operator observed the subjects and the EEG traces, alerting the subject on signs of behavioral and/or EEG drowsiness to maintain the resting EEG as stable as possible. Each recording lasted approximately 2 min, during which time the subject's eyes were closed. 10-s-long EEG segments free of artifacts, such as ocular and muscle movements, were selected and down-sampled to 256 Hz for further analysis.

C. PNES Discrimination Based on the Common Spatial Pattern of the Weighted Connectivity Network

The brain network can be used to describe the connectivity among multiple regions [11], [27], [28], [39]. Various studies using sMRI and fMRI have shown that patients with epilepsy

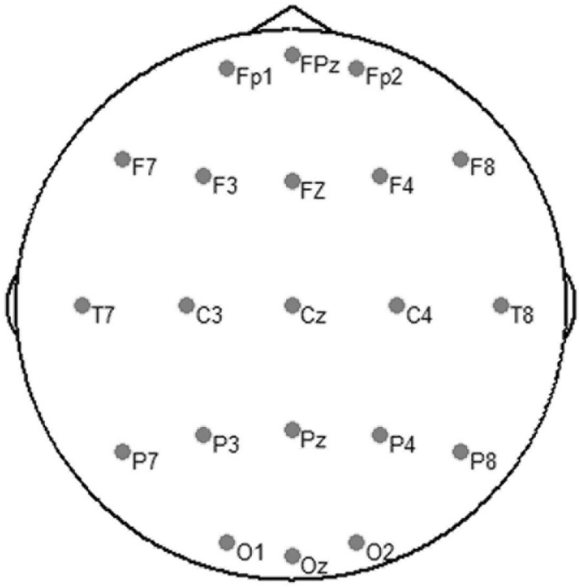

Fig. 1. Twenty-one 10–20 canonical electrode montage used for network analysis.

have different connectivity than normal individuals [20], [21]; these alterations suggest the potential to classify patients with epilepsy using brain network information. Considering that the main challenge for PNES discrimination is that the differences in network statistical properties between PNES and other types of epilepsy are minor, we present a new method, SPN, to further extract the implicit information contained in the spatial topology of the brain network.

EEG-based network analysis is inevitably influenced by the volume conduction and reference effect [39]–[42]. In this study, to lower the non-zero reference effect, the data were first transformed to the approximate zero reference using REST (http://www.neuro.uestc.edu.cn/REST/) [39]. To lower the effect of volume conduction, the 21 canonical electrodes of the 10–20 system were selected from a total of 60 electrodes to construct the brain network [39]. The montage of the 21 10–20 canonical electrodes used is shown in Fig. 1.

1) Linkage Strength of the Nodes: Coherence (Coh) is the most commonly used method of analyzing the cooperative, synchrony-defined cortical neuronal assemblies; this method represents the linear relationship at a specific frequency between two signals $x(t)$ and $y(t)$ based on their cross-spectrum. In this study, we adopted frequency-specific coherence to denote the linkage strength between two network nodes. Coh is expressed as follows [43]:

$$C_{\mathrm{XY}}(f) = \frac{|P_{\mathrm{XY}}(f)|^2}{P_{\mathrm{XX}}(f)P_{\mathrm{YY}}(f)} \tag{1}$$

where $P_{\mathrm{XY}}(f)$ is the cross-spectrum of $x(t)$ and $y(t)$ at frequency f, and $P_{\mathrm{XX}}(f)$ and $P_{\mathrm{YY}}(f)$ indicate the autospectra at frequency f, estimated from the Welch-based spectrum at 0.1 Hz resolution. Based on the frequency-dependent coherence $C_{\mathrm{XY}}(f)$, the edge linkages in the relevant frequency bands, including theta (4–8 Hz), alpha (8–13 Hz), beta (13–30 Hz), gamma (30–40 Hz), and the full band (4–60 Hz), were estimated by averaging the coherence strength within the relevant frequency band. After calculating the paired coherence between each pair of 21 electrodes, the 21×21 weighted adjacency (connectivity) matrix was constructed to denote interactions among the 21 nodes in a certain frequency band.

2) Network Properties: The brain network was constructed based on the 21×21 weighted adjacency (connectivity) matrix using the corresponding coherence as the edge linkage c_{ij} between two nodes i and j. After constructing the weighted network, the clustering coefficients and the shortest path length were used to measure the local and global information processing ability of the brain, respectively. The (weighted) clustering index of vertex i is defined as [27]:

$$C_i = \frac{\sum\limits_{k\neq i}\sum\limits_{\substack{l\neq i\\ l\neq k}} c_{ik}c_{il}c_{kl}}{\sum\limits_{k\neq i}\sum\limits_{\substack{l\neq i\\ l\neq k}} c_{ik}c_{il}} \tag{2}$$

where c_{ij} is the edge linkage strength between vertices i and j obtained by (1). The mean clustering coefficient (C) of the entire weighted network was then determined as follows:

$$C = \frac{1}{N}\sum_{i=1}^{N} C_i. \tag{3}$$

Regarding the weighted network, the length of an edge between vertices i and j is the inverse of the aforementioned edge weight [27],

$$L_{ij} = \begin{cases} 1/c_{ij}, & \text{if} \quad c_{ij} \neq 0 \\ 1, & \text{if} \quad c_{ij} = 0 \end{cases}. \tag{4}$$

Therefore, the length of a weighted path between two vertices is defined as the sum of the lengths of the edges of this path. Similarly, the average weighted path length of the entire graph (L) was computed as

$$L = \frac{1}{(1/N(N-1))\sum\limits_{i=1}^{N}\sum\limits_{j\neq i}^{N}(1/L_{ij})}. \tag{5}$$

3) Network Analysis: The described network analysis procedure was performed for the 10-s-long segment of each subject, resulting in one connectivity (adjacency) matrix with a dimension of 21×21 for each subject. Based on the connectivity matrix, the network topology and properties were calculated for each subject in different frequency bands. The differences in network properties (the clustering coefficients and shortest path length) between groups were evaluated using the two-sample t test. The network properties and spatial topology were then used in the following procedure to perform the corresponding classification in different applications.

4) Common Spatial Pattern of the Weighted Connectivity Network: Assuming that the inherent network characteristics of PNES and epilepsy subjects may provide a potential mechanism to discern these disorders, we used the common SPN to refine the inherent and implicit spatial information in the adjacency matrix to differentiate PNES from epilepsy. The basic

concept of SPN is to identify a group of spatial filters that maximize the variance of one class while minimizing that of another class [32], [33], [44], [45]. The crucial goal of SPN is to identify the common spatial pattern of various weighted brain network topologies; thus, the spatial pattern extracted by SPN is in the network space and not in the physical data space, as is the case with canonical CSP.

Let ϕ_1 and ϕ_2 be the 21×21 adjacency matrices for PNES and epilepsy subjects, respectively. The spatial filters are the projections, the form of which is equivalent to maximizing the following function:

$$J(w) = \frac{w^T \phi_1^T \phi_1 w}{w^T \phi_2^T \phi_2 w} = \frac{w^T \Phi_1 w}{w^T \Phi_2 w} \tag{6}$$

where Φ_1 and Φ_2 are the covariance matrix of the adjacency matrix for the two groups. Note that the scaling of the projection w will have no effect on the object value; hence, (6) can be transformed into a constrained optimization problem as follows:

$$\begin{cases} \arg\max\limits_{w} \ w^T \Phi_1 w \\ \text{subject to } w^T \Phi_2 w = 1 \end{cases}. \tag{7}$$

By introducing the Lagrange multiplier, the objective function can be rewritten as

$$L(w; \lambda) = w^T \Phi_1 w - \lambda (w^T \Phi_2 w - 1). \tag{8}$$

By taking the derivative of (8) with respect to w under the condition $\frac{\partial L}{\partial w} = 0$, the objective projection w can be estimated using the generalized eigenvalue equation,

$$\Phi_1 w = \lambda \Phi_2 w \tag{9}$$

where λ denotes the eigenvalue of the generalized eigenvalue equation and w is the corresponding eigenvector [46]. Regarding the multiple m spatial filters, (9) can be solved as

$$\Phi_2^{-1} \Phi_1 W = \sum W \tag{10}$$

where W is the matrix consisting of the eigenvectors of $\Phi_2^{-1}\Phi_1$ and $\sum = \mathrm{diag}(\lambda_1, \lambda_2, ..., \lambda_m)$, with λ being the corresponding singular values. For example, when the most discriminative three pairs of CSP filters are used, six-dimensional spatial features will be obtained [45], [47], [48]. Specifically, the three pairs of discriminative CSP filters comprises a matrix $W_{\mathrm{csp}} = [\mathrm{Filter1}, \mathrm{Filter2}, ..., \mathrm{Filter6}]$, with each filter being a 21-length vector, i.e., W_{csp} with a dimension of 21×6. The differentiation abilities of the filters were denoted by the eigenvalues in $\sum$, and the first and last filters corresponding to the largest and smallest eigenvalues consist of the most discriminative CSP filter pair [48]. For a 21×21 connectivity matrix ϕ, the corresponding CSP feature transformation is $F_{\mathrm{csp}} = \log(\mathrm{var}(W_{\mathrm{csp}}^T \phi))$, which results in a vector of length 6. In this study, we tested the classification performance using two, four, and six SPN features.

The connectivity matrix constructed from the coherence is the second-order measurement of the signal, and the corresponding covariance matrix of the connectivity matrix is the fourth-order measurement of the signal. Therefore, the common spatial pattern extracted the fourth-order information of the EEG signal to perform the classification.

5) PNES Differentiation Based on SPN: In the clinic, both epilepsy and PNES patients can be reliably and accurately distinguished from a group of normal subjects based on their abnormal behavior; therefore, we established the procedure based on SPN to differentiate PNES and epilepsy. The detailed classification procedure is depicted in Fig. 2.

Based on the 21×21 adjacency matrices derived from PNES and epilepsy, several SPN filters were estimated according to (6)–(9).

SPN filters were then applied to the training set to extract the corresponding features. Fisher discriminate analysis (FDA) and support vector machine (SVM) classifier with default parameters were trained by the extracted features for the classification. The detailed default parameters used for SVM were 1.0 for C and $1/k$ for the radial basis variance, with k being the number of samples in the training set.

After the adjacency matrix was calculated based on the Resting EEG for classification, the SPN filters estimated in the training procedure were used to extract the spatial network topology information from the corresponding adjacency matrix [see Fig. 2(b)]. Based on the SPN features, the trained classifier was then used for the final differentiation.

6) Evaluation Indices: To evaluate the classification performance, the accuracy (Acc), sensitivity (Sen), and specificity (Spe) were used, and the detailed calculations for the three metrics were as follows:

$$\begin{aligned} \mathrm{Acc} &= \frac{n_{\mathrm{PNES}} + n_{\mathrm{Epilepsy}}}{N_{\mathrm{PNES}} + N_{\mathrm{Epilepsy}}} \times 100\% \\ \mathrm{Sen} &= \frac{n_{\mathrm{PNES}}}{N_{\mathrm{PNES}}} \times 100\% \\ \mathrm{Spe} &= \frac{n_{\mathrm{Epilepsy}}}{N_{\mathrm{Epilepsy}}} \times 100\% \end{aligned} \tag{11}$$

where N_{PNES} and N_{Epilepsy} are the actual number of PNES and epilepsy patients, respectively (i.e., 15 and 10), and n_{PNES} and n_{Epilepsy} are the correctly predicted number of PNES and epilepsy patients, respectively.

III. Results

The two network property values averaged across the subjects for the PNES, epilepsy, and normal groups are shown in Tables I and II.

As shown in Tables I and II, both the clustering coefficients and the shortest path length were significantly different in the gamma and full-frequency bands between the patients (PNES and epilepsy) and the normal subjects. These two tables further reveal that the network properties between the PNES and epilepsy groups were not significantly different. This finding indicates the difficulty in classifying PNES and epilepsy based only on network properties where a low classification performance is reported (see Table III). Considering that the current dataset is relatively small, the leave-one-out strategy [31], [49] was adopted to evaluate the classification performance.

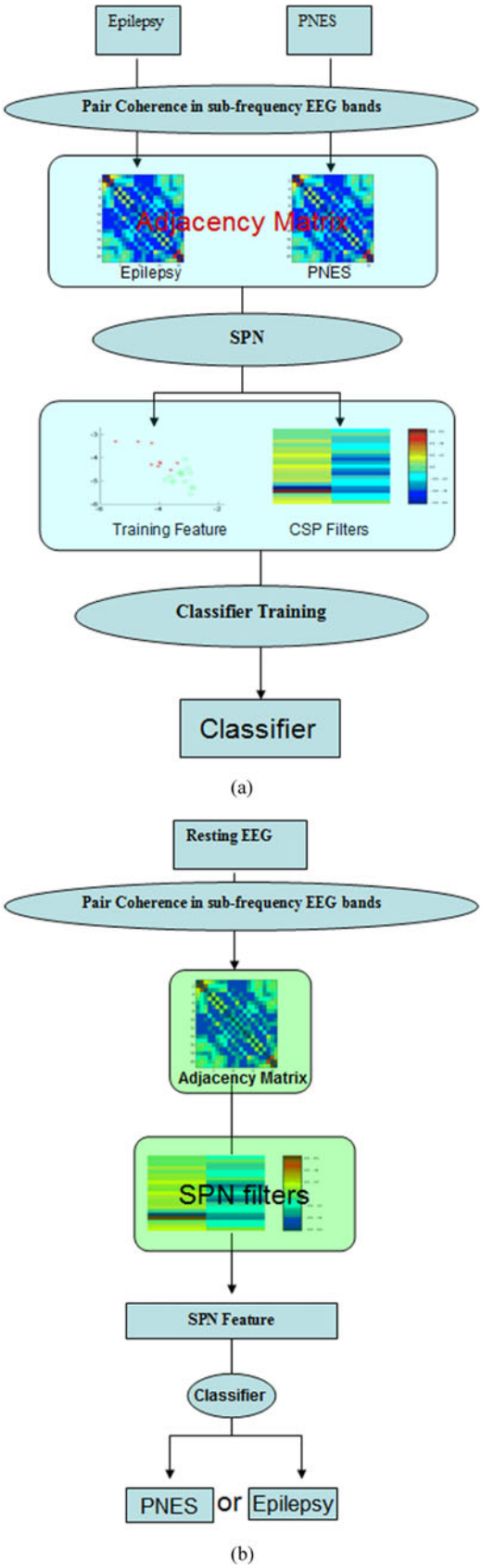

Fig. 2. Training and classification procedure for differentiation between PNES and epilepsy: (a) training; (b) classification.

TABLE I
CLUSTERING COEFFICIENTS AMONG THE THREE GROUPS

Frequency band	PNES Mean±SD	Epilepsy Mean±SD	Normal Mean±SD	Patient vs. Normal *p*-value
theta	0.27±0.07	0.32±0.04	0.32±0.05	0.2004
alpha	0.41±0.14	0.42±0.09	0.49±0.12	0.0631
beta	0.21±0.04	0.23±0.02	0.25±0.04	0.0127
gamma	0.16±0.03	0.15±0.02	0.20±0.04	0.0003
all bands	0.20±0.02	0.20±0.02	0.26±0.03	0.00003

TABLE II
SHORTEST PATH LENGTH AMONG THE THREE GROUPS

Frequency band	PNES Mean±SD	Epilepsy Mean±SD	Normal Mean±SD	Patient vs. Normal *p*-value
theta	3.72±0.72	3.25±0.58	3.22±0.43	0.1334
alpha	2.91±0.99	2.72±0.62	2.36±0.66	0.0713
beta	4.74±0.78	4.45±0.71	4.08±0.61	0.0236
gamma	6.82±1.67	7.29±1.67	5.47±1.26	0.0038
all bands	5.17±0.73	5.16±0.84	4.33±0.63	0.0010

The adjacency matrix contains the spatial information required to denote interactions between brain areas, and the implicit and inherent spatial information of the PNES and epilepsy groups may be contained in the spatial patterns. We have provided the corresponding information for the SPN filter in the beta frequency band as an example to show how SPN can extract the discriminative spatial information in brain networks. SPNs in other frequency bands have similar working mechanisms to that in the beta band.

Fig. 3 shows the six most discriminative SPN filters identified from the adjacency matrix of the PNES and epilepsy groups in the beta frequency band.

The corresponding filter topology on the head surface for the two most discriminative filters (Filters 1 and 6) are given in Fig. 4(a), and the difference in the network topology between the PNES and epilepsy groups is shown in Fig. 4(b), in which the Kruskal-Wallis test [50] was used to evaluate the difference for each edge and only those edges with a statistically significant difference ($p < 0.05$) are shown.

Fig. 5 is a scatter plot of the two SPN features that are the most discriminative between the PNES and epilepsy groups in the beta frequency band.

Table IV lists the corresponding discrimination performance, including the accuracy (ACC), sensitivity (SEN), and specificity (SPE), for the PNES and epilepsy groups in different frequency bands based on the SPN features extracted using 2, 4, and 6 filters, respectively. Using the SPN spatial filters, the discrimination performance in all concerned frequency bands was significantly improved compared to those listed in Table III, i.e., those based on the network statistical properties. Table IV also reveals that SPN filter number affected the classification performance.

TABLE III
DIFFERENTIATION PERFORMANCE (%) BETWEEN THE PNES AND EPILEPSY GROUPS BASED ON NETWORK PROPERTIES

	Frequency band (Hz)	theta(4-8)	alpha(8-13)	beta(13-30)	gamma(30-60)	all bands(4-60)
SVM	ACC(%)	68.00	56.00	36.00	40.00	40.00
	SEN(%)	73.33	60.00	13.00	0.00	0.00
	SPE(%)	60.00	50.00	70.00	100.00	100.00
FDA	ACC(%)	72.00	56.00	40.00	48.00	44.00
	SEN(%)	86.67	93.33	66.67	80.00	73.33
	SPE(%)	50.00	0.00	0.00	0.00	0.00

TABLE IV
DIFFERENTIATION PERFORMANCE FOR THE PNES AND EPILEPSY GROUPS IN VARIOUS FREQUENCY BANDS BASED ON SPN USING 2, 4, AND 6 FILTERS

2 filters

	Frequency band (Hz)	theta(4-8)	alpha(8-13)	beta(13-30)	gamma(30-60)	all bands(4-60)
SVM	ACC(%)	76.00	60.00	**88.00**	64.00	**88.00**
	SEN(%)	73.33	66.66	**93.33**	80.00	**93.33**
	SPE(%)	80.00	50.00	**80.00**	40.00	**80.00**
FDA	ACC(%)	76.00	72.00	**84.00**	64.00	**84.00**
	SEN(%)	86.66	66.66	**93.33**	66.67	**93.33**
	SPE(%)	60.00	80.00	**70.00**	60.00	**70.00**

4 filters

	Frequency band (Hz)	theta(4-8)	alpha(8-13)	beta(13-30)	gamma(30-60)	all bands(4-60)
SVM	ACC(%)	76.00	72.00	**88.00**	76.00	80.00
	SEN(%)	80.00	80.00	**93.33**	86.67	93.33
	SPE(%)	70.00	60.00	**80.00**	60.00	60.00
FDA	ACC(%)	72.00	84.00	**88.00**	76.00	80.00
	SEN(%)	80.00	80.00	**93.33**	80.00	93.33
	SPE(%)	60.00	90.00	**80.00**	70.00	60.00

6 filters

	Frequency band (Hz)	theta(4-8)	alpha(8-13)	beta(13-30)	gamma(30-60)	all bands(4-60)
SVM	ACC(%)	76.00	84.00	**92.00**	76.00	80.00
	SEN(%)	86.67	93.33	**100.00**	86.67	93.33
	SPE(%)	60.00	70.00	**80.00**	60.00	60.00
FDA	ACC(%)	72.00	**88.00**	**88.00**	80.00	72.00
	SEN(%)	86.67	**86.67**	**93.33**	86.67	86.67
	SPE(%)	50.00	**90.00**	**80.00**	70.00	50.00

*Bold values indicate the best performance in those frequency bands for the corresponding classifier.

IV. DISCUSSION

Tables I and II show that the PNES and epilepsy subjects had decreased clustering coefficients and an increased shortest path length compared to the normal subjects in the frequency bands of interest; this may be an indicator of impaired local information processing and global information integration in patients [26], [28]. PNES has been shown to correlate with functional and structural brain network alterations using MRI-related studies [22]. Recent scalp EEG-based studies have also revealed that PNES might lack a relatively long linkage in the brain network topology, indicating the impairment of information transferring and processing [51]. In practice, PNES and epilepsy patients can be easily discerned from normal subjects based on their abnormal behavior [5], [19], [25], [35]. The main challenge

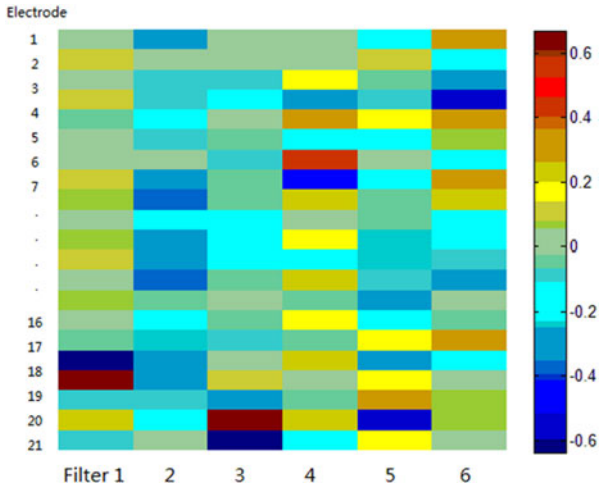

Fig. 3. Six most discriminative SPN filters in the beta band. Each column represents one spatial filter, and the vertical axis is the node index. The colors denote the different weights imposed on the different electrode nodes.

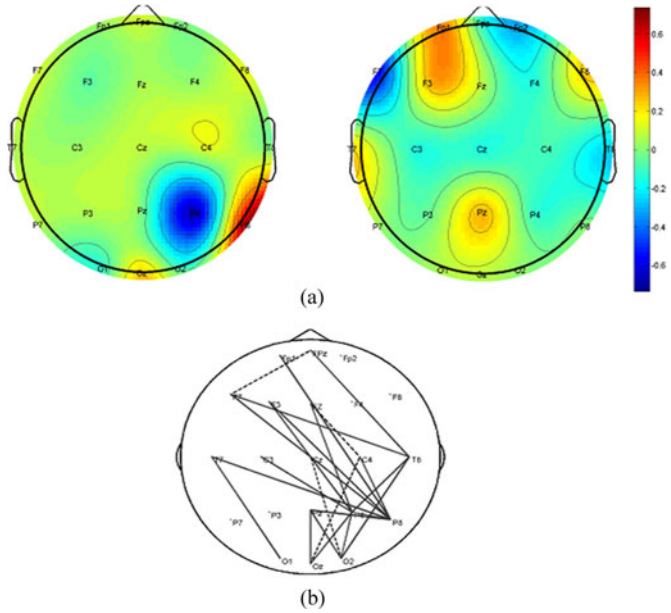

Fig. 4. The scalp topologies for the most distinct SPN filters (Filters 1 and 6) and the topology difference in the network between the PNES and epilepsy groups in the beta band. (a) The scalp topology of the two most distinct SPN filters; (b) the network topology difference between the PNES and epilepsy groups. The solid lines in (b) denote significantly increased linkage strength ($p < 0.05$) between the PNES and epilepsy groups; the dashed lines denote significantly decreased linkage strength ($p < 0.05$).

for PNES discrimination is the higher classification error of misclassifying PNES as other epilepsies, which might affect subsequent clinical intervention [2], [5], [6], [13], [17]. Tables I and II also show that the network properties between PNES and epilepsy are very close, which results in a very low classification performance based on the network properties, as revealed in Table III. Essentially, the network statistical properties are the direct statistical measurements of the networks, and these cannot encompass the entire information content related to the network topology. As shown in Fig. 6, the two network topologies vary in the bilateral hemisphere, whereas the network properties, such

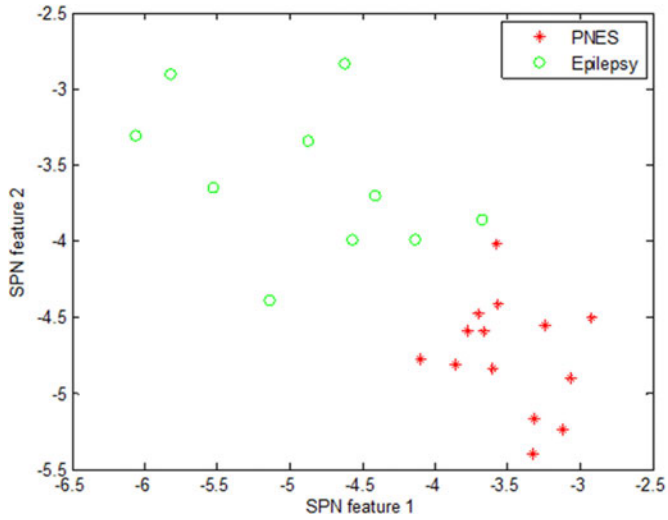

Fig. 5. Scatter plot of the two SPN features that are the most discriminative between the PNES and epilepsy groups in the beta frequency band.

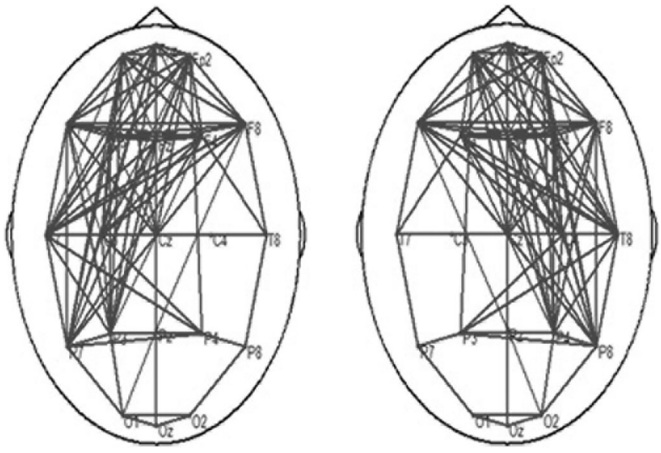

Fig. 6. Two networks with different topology structures but the same network property values.

as clustering coefficients and the shortest path length, are the same for the two networks. Therefore, the network properties fail to capture the spatial differentiation information in the networks.

In fact, PNES and epilepsy patients may be more readily discriminated in terms of network topology structure as shown in Fig. 4(b). In previous studies [38], [52], researchers used structural MRI to reveal that PNES was less detected with brain structural abnormalities in the frontal and temporal areas compared to epileptic subjects. The network topology difference in Fig. 4(b) shows that subjects with PNES have stronger linkages between the frontal area and the temporal/occipital areas than subjects in the epilepsy group, which is consistent with the structural abnormality difference between the two groups. Combining the topology differences in Fig. 4(b) and the statistical properties in Tables I and II, we see that although a clear difference in spatial topology exists in Fig. 4(b), the statistical network properties did not reflect any significant difference. Here, we successfully found that the SPN can extract the inherent spatial topology information in these two patient groups.

As shown in Fig. 3, the SPN filters impose different weights on the adjacency matrix to emphasize the electrode nodes exhibiting a significant difference with larger coefficients while compressing the nodes without clear differences with smaller coefficients between the two groups. The working mechanisms of SPN are further revealed in Fig. 4, which shows that the SPN filters capture the differentiating spatial network information in the brain network. This result was accomplished by providing larger weights to network nodes exhibiting significant linkage differences between the PNES and epilepsy groups. Thus, the nodes exhibiting large topology differences were those possessing significant SPN weights. Fig. 5 further reveals that after SPN transformation, the two groups can be adequately discriminated based on the first two discriminative SPN features. The classification performance in Table IV achieved for the various SPN filter numbers is consistently better than the classification performance in Table III, based on the network properties in each frequency band. The highest classification performance (92% accuracy, 100% sensitivity, and 80% specificity) can be achieved when the six SPN features in the beta band are considered for classification. The use of six SPN features can capture more differentiating information than the use of two and four SPN features, resulting in a more reliable classification, as shown in other disciplines, such as BCI [45], [47], [48]. Therefore, in the actual application, we propose to use six SPN filters to extract the spatial network topology information. Here, only the network properties including clustering coefficients and the shortest path length were tested for their ability to distinguish between PNES and epilepsy, whereas other metrics, such as the modularity and smallworldness that have previously been demonstrated to correlate with PNES seizure frequency [53], may provide more reliable classification. However, these statistical network properties, although essentially derived from the network topology structure, still may miss the important spatial information, but the spatial information contained in the topology structure may be more important for distinguishing between PNES and epilepsy, as shown by the SPN results.

Essentially, SPN performs similarly to a sub-network-seeking filter that has the ability to automatically select modules having clear spatial differences between PNES and epilepsy in the brain network space by giving them a larger emphasis while compressing other modules by providing them with smaller coefficients. Therefore, the difference in spatial topology exhibited between PNES and epilepsy subjects can be adequately extracted using such a band-pass-like filter, resulting in a more reliable differentiation. Coherence is influenced by volume conduction; other techniques, such as coherency index [40] and current source density (CSD) [54], that are less influenced by the volume conduction effect may be more meaningful for this type of EEG-based network analysis. Irrespective of the technique used for volume conduction reduction, SPN can still be used to extract the spatial information contained in the brain's network structure.

The difficulty for classification between PNES and other epileptic seizures is mainly due to the very limited knowledge regarding the underlying neural mechanism of PNES [2], [6], [38]; hence, more reliable recognition will require further research on the related neural mechanism. This study is subject to several limitations; first, the number of subjects used was relatively small, which is a common problem in most of the related studies on PNES [2]. In future, we will expand the proposed approach to a greater number of subjects exhibiting several types of epilepsies. Second, this paper did not consider the use of feature selection criteria to combine the complementary information in different frequency bands, which might further improve the classification performance.

V. Conclusion

Based on the resting scalp EEG, the proposed classification can robustly and reliably differentiate between PNES and epilepsy subjects. The differentiation was based on the common SPN derived from the brain network space of the resting scalp EEG. The newly developed SPN is a fourth-order measure of the original resting scalp EEG data and can extract the inherent spatial information in the resting network, facilitating the reliable recognition of PNES relative to local epilepsy subjects. This method may be helpful for clinicians aiming to discover implicit information during the diagnosis of PNES.

Acknowledgment

The authors would like to thank the anonymous reviewers for their insightful comments, which have improved their work.

References

[1] N. Bodde, J. Brooks, G. Baker, P. Boon, J. Hendriksen, O. Mulder, and A. Aldenkamp, "Psychogenic non-epileptic seizures–definition, etiology, treatment and prognostic issues: A critical review," *Seizure: J. Brit. Epilepsy Assoc.*, vol. 18, no. 8, pp. 543–553, 2009.

[2] P. Dickinson and K. J. Looper, "Psychogenic nonepileptic seizures: A current overview," *Epilepsia*, vol. 53, no. 10, pp. 1679–1689, 2012.

[3] J. Kuyk, F. Leijten, H. Meinardi, P. Spinhoven, and R. V. Dyck, "The diagnosis of psychogenic non-epileptic seizures: A review," *Seizure*, vol. 6, no. 4, pp. 243–253, 1997.

[4] M. Reuber and C. E. Elger, "Psychogenic nonepileptic seizures: Review and update," *Epilepsy Behav.*, vol. 4, no. 3, pp. 205–216, 2003.

[5] T. U. Syed, W. C. LaFrance, E. S. Kahriman, S. N. Hasan, V. Rajasekaran, D. Gulati, S. Borad, A. Shahid, G. Fernandez-Baca, and N. Garcia, "Can semiology predict psychogenic nonepileptic seizures? A prospective study," *Ann. Neurol.*, vol. 69, no. 6, pp. 997–1004, 2011.

[6] N. Bodde, J. Brooks, G. Baker, P. Boon, J. Hendriksen, and A. Aldenkamp, "Psychogenic non-epileptic seizures—diagnostic issues: A critical review," *Clin. Neurol. Neurosurg.*, vol. 111, no. 1, pp. 1–9, 2009.

[7] F. M. Cuthill and C. A. Espie, "Sensitivity and specificity of procedures for the differential diagnosis of epileptic and non-epileptic seizures: A systematic review," *Seizure*, vol. 14, no. 5, pp. 293–303, 2005.

[8] S. W. Hill and S. D. Gale, "Predicting psychogenic nonepileptic seizures with the personality assessment inventory and seizure variables," *Epilepsy Behav.*, vol. 22, no. 3, pp. 505–510, 2011.

[9] W. C. LaFrance and S. R. Benbadis, "Avoiding the costs of unrecognized psychological nonepileptic seizures," *Neurology*, vol. 66, no. 11, pp. 1620–1621, 2006.

[10] G. Baslet, "Psychogenic non-epileptic seizures: A model of their pathogenic mechanism," *Seizure*, vol. 20, no. 1, pp. 1–13, 2011.

[11] S. J. van der Kruijs, N. M. Bodde, M. J. Vaessen, R. H. Lazeron, K. Vonck, P. Boon, P. A. Hofman, W. H. Backes, A. P. Aldenkamp, and J. F. Jansen, "Functional connectivity of dissociation in patients with psychogenic non-epileptic seizures," *J. Neurol., Neurosurg. Psychiatry*, vol. 83, no. 3, pp. 239–247, 2012.

[12] A. Avbersek and S. Sisodiya, "Does the primary literature provide support for clinical signs used to distinguish psychogenic nonepileptic seizures from epileptic seizures?" *J. Neurol., Neurosurg. Psychiatry*, vol. 81, no. 7, pp. 719–725, 2010.

[13] N. Bodde, S. van der Kruijs, D. Ijff, R. Lazeron, K. Vonck, P. Boon, and A. Aldenkamp, "Subgroup classification in patients with psychogenic non-epileptic seizures," *Epilepsy Behav.*, vol. 26, no. 3, pp. 279–289, 2012.
[14] L. H. Goldstein and J. D. Mellers, "Recent developments in our understanding of the semiology and treatment of psychogenic nonepileptic seizures," *Curr. Neurol. Neurosci. Rep.*, vol. 12, no. 4, pp. 436–444, 2012.
[15] E. W. Massey and L. C. McHenry, Jr., "Hysteroepilepsy in the nineteenth century: Charcot and Gowers," *Neurology*, vol. 36, no. 1, pp. 65–67, Jan. 1986.
[16] C. Hubsch, C. Baumann, C. Hingray, N. Gospodaru, J.-P. Vignal, H. Vespignani, and L. Maillard, "Clinical classification of psychogenic non-epileptic seizures based on video-EEG analysis and automatic clustering," *J. Neurol., Neurosurg. Psychiatry*, vol. 82, no. 9, pp. 955–960, 2011.
[17] T. Syed, A. Arozullah, K. Loparo, R. Jamasebi, G. Suciu, C. Griffin, R. Mani, I. Syed, T. Loddenkemper, and A. Alexopoulos, "A self-administered screening instrument for psychogenic nonepileptic seizures," *Neurology*, vol. 72, no. 19, pp. 1646–1652, 2009.
[18] W. C. LaFrance and S. Plioplys, "Neuropsychiatric disorders: Does semiology of psychogenic nonepileptic seizures matter?" *Nature Rev. Neurol.*, vol. 8, no. 6, pp. 302–303, 2012.
[19] J. A. Pillai and S. R. Haut, "Patients with epilepsy and psychogenic non-epileptic seizures: An inpatient video-EEG monitoring study," *Seizure*, vol. 21, no. 1, pp. 24–27, 2012.
[20] C. Luo, Q. Li, Y. Lai, Y. Xia, Y. Qin, W. Liao, S. Li, D. Zhou, D. Yao, and Q. Gong, "Altered functional connectivity in default mode network in absence epilepsy: A resting-state fMRI study," *Human Brain Mapp.*, vol. 32, no. 3, pp. 438–449, 2011.
[21] C. Luo, Q. Li, Y. Xia, X. Lei, K. Xue, Z. Yao, Y. Lai, W. Liao, D. Zhou, and P. A. Valdes-Sosa, "Resting state basal ganglia network in idiopathic generalized epilepsy," *Human Brain Mapp.*, vol. 33, no. 6, pp. 1279–1294, 2012.
[22] J. R. Ding, D. An, W. Liao, J. Li, G. R. Wu, Q. Xu, Z. Long, Q. Gong, D. Zhou, O. Sporns, and H. Chen, "Altered functional and structural connectivity networks in psychogenic non-epileptic seizures," *PloS one*, vol. 8, no. 5, p. e63850, 2013.
[23] R. Duncan and M. Oto, "Predictors of antecedent factors in psychogenic nonepileptic attacks Multivariate analysis," *Neurology*, vol. 71, no. 13, pp. 1000–1005, 2008.
[24] K. A. McNally, B. K. Schefft, J. P. Szaflarski, S. R. Howe, H.-S. Yeh, and M. D. Privitera, "Application of signal detection theory to verbal memory testing to distinguish patients with psychogenic nonepileptic seizures from patients with epileptic seizures," *Epilepsy Behav.*, vol. 14, no. 4, pp. 597–603, 2009.
[25] B. Mostacci, F. Bisulli, L. Alvisi, L. Licchetta, A. Baruzzi, and P. Tinuper, "Ictal characteristics of psychogenic nonepileptic seizures: What we have learned from video/EEG recordings—A literature review," *Epilepsy Behav.*, vol. 22, no. 2, pp. 144–153, 2011.
[26] M. D. Fox and M. E. Raichle, "Spontaneous fluctuations in brain activity observed with functional magnetic resonance imaging," *Nature Rev. Neurosci.*, vol. 8, no. 9, pp. 700–711, 2007.
[27] C. Stam, W. De Haan, A. Daffertshofer, B. Jones, I. Manshanden, A. M. C. van Walsum, T. Montez, J. Verbunt, J. De Munck, and B. Van Dijk, "Graph theoretical analysis of magnetoencephalographic functional connectivity in Alzheimer's disease," *Brain*, vol. 132, no. 1, pp. 213–224, 2009.
[28] C. Stam, Y. Van der Made, Y. Pijnenburg, and P. Scheltens, "EEG synchronization in mild cognitive impairment and Alzheimer's disease," *Acta Neurologica Scandinavica*, vol. 108, no. 2, pp. 90–96, 2003.
[29] L. Liu, L.-L. Zeng, Y. Li, Q. Ma, B. Li, H. Shen, and D. Hu, "Altered cerebellar functional connectivity with intrinsic connectivity networks in adults with major depressive disorder," *PloS One*, vol. 7, no. 6, p. e39516, 2012.
[30] H. Shen, L. Wang, Y. Liu, and D. Hu, "Discriminative analysis of resting-state functional connectivity patterns of schizophrenia using low dimensional embedding of fMRI," *Neuroimage*, vol. 49, no. 4, p. 3110, 2010.
[31] L.-L. Zeng, H. Shen, L. Liu, L. Wang, B. Li, P. Fang, Z. Zhou, Y. Li, and D. Hu, "Identifying major depression using whole-brain functional connectivity: A multivariate pattern analysis," *Brain*, vol. 135, no. 5, pp. 1498–1507, 2012.
[32] Z. Koles, J. Lind, and P. Flor-Henry, "Spatial patterns in the background EEG underlying mental disease in man," *Electroencephalogr. Clin. Neurophysiol.*, vol. 91, no. 5, p. 319, 1994.
[33] Z. J. Koles, M. S. Lazar, and S. Z. Zhou, "Spatial patterns underlying population differences in the background EEG," *Brain Topogr.*, vol. 2, no. 4, pp. 275–284, 1990.
[34] E. Beghi, A. Carpio, L. Forsgren, D. C. Hesdorffer, K. Malmgren, J. W. Sander, T. Tomson, and W. A. Hauser, "Recommendation for a definition of acute symptomatic seizure," *Epilepsia*, vol. 51, no. 4, pp. 671–675, 2010.
[35] R. S. Fisher, W. V. E. Boas, W. Blume, C. Elger, P. Genton, P. Lee, and J. Engel, "Epileptic seizures and epilepsy: Definitions proposed by the International League Against Epilepsy (ILAE) and the International Bureau for Epilepsy (IBE)," *Epilepsia*, vol. 46, no. 4, pp. 470–472, 2005.
[36] T. R. Henry, "seizures and Epilepsy: Pathophysiology and principles of diagnosis," *Hospital Phys. Epilepsy Board Rev. Manual*, vol. 1, Part 1, pp. 1–21, 2012.
[37] S. R. Benbadis, K. Siegrist, W. O. Tatum, L. Heriaud, and K. Anthony, "Short-term outpatient EEG video with induction in the diagnosis of psychogenic seizures," *Neurology*, vol. 63, no. 9, pp. 1728–1730, Nov. 9, 2004.
[38] O. Devinsky, D. Gazzola, and W. C. LaFrance, "Differentiating between nonepileptic and epileptic seizures," *Nature Rev. Neurol.*, vol. 7, pp. 210–220, 2011.
[39] Y. Qin, P. Xu, and D. Yao, "A comparative study of different references for EEG default mode network: The use of the infinity reference," *Clin. Neurophysiol.*, vol. 121, no. 12, p. 1981, 2010.
[40] L. Marzetti, G. Nolte, M. Perrucci, G. Romani, and C. D. Gratta, "The use of standardized infinity reference in EEG coherency studies," *Neuroimage*, vol. 36, no. 1, pp. 48–63, 2007.
[41] P. L. Nunez, R. B. Silberstein, Z. Shi, M. R. Carpenter, R. Srinivasan, D. M. Tucker, S. M. Doran, P. J. Cadusch, and R. S. Wijesinghe, "EEG coherency II: Experimental comparisons of multiple measures," *Clin. Neurophysiol.*, vol. 110, no. 3, pp. 469–486, Mar. 1999.
[42] C. J. Stam, Y. van der Made, Y. A. Pijnenburg, and P. Scheltens, "EEG synchronization in mild cognitive impairment and Alzheimer's disease," *Acta Neurol. Scand.*, vol. 108, no. 2, pp. 90–96, Aug. 2003.
[43] L. H. Koopmans, *The Spectral Analysis of Time Series*. New York: Academic, 1995.
[44] B. Blankertz, R. Tomioka, S. Lemm, M. Kawanabe, and K. R. Muller, "Optimizing spatial filters for robust EEG single-trial analysis," *IEEE Signal Process. Mag.*, vol. 25, no. 1, pp. 41–56, Jan. 2008.
[45] P. Xu, P. Yang, X. Lei, and D. Yao, "An enhanced probabilistic LDA for multi-class brain computer interface," *PloS One*, vol. 6, no. 1, p. e14634, 2011.
[46] B. Blankertz, G. Dornhege, M. Krauledat, K.-R. Müller, and G. Curio, "The non-invasive Berlin Brain–Computer Interface: Fast acquisition of effective performance in untrained subjects," *Neuroimage*, vol. 37, no. 2, pp. 539–550, 2007.
[47] B. Blankertz, G. Dornhege, M. Krauledat, K.-R. Müller, and G. Curio, "The non-invasive Berlin Brain-Computer Interface: Fast acquisition of effective performance in untrained subjects," *Neuroimage*, vol. 37, no. 2, pp. 539–550, 2007.
[48] B. Blankertz, R. Tomioka, S. Lemm, M. Kawanabe, and K.-R. Muller, "Optimizing spatial filters for robust EEG single-trial analysis," *Signal Process. Mag., IEEE*, vol. 25, no. 1, pp. 41–56, 2008.
[49] P. Xu, M. Kasprowicz, M. Bergsneider, and X. Hu, "Improved noninvasive intracranial pressure assessment with nonlinear kernel regression," *IEEE Trans. Inf. Technol. Biomed.*, vol. 14, no. 4, pp. 971–978, 2010.
[50] S. D. Shorvon, A. Löwenthal, D. Janz, E. Bielen, and P. Loiseau, "Multicenter double-blind, randomized, placebo-controlled trial of levetiracetam as add-on therapy in patients with refractory partial seizures," *Epilepsia*, vol. 41, no. 9, pp. 1179–1186, 2000.
[51] Q. Xue, Z. Y. Wang, X. C. Xiong, C. Y. Tian, Y. P. Wang, and P. Xu, "Altered brain connectivity in patients with psychogenic non-epileptic seizures: A scalp electroencephalography study," *J. Int. Med. Res.*, vol. 41, no. 5, pp. 1682–1690, Oct. 2013.
[52] M. Reuber, G. Fernandez, C. Helmstaedter, A. Qurishi, and C. E. Elger, "Evidence of brain abnormality in patients with psychogenic nonepileptic seizures," *Epilepsy Behav.*, vol. 3, no. 3, pp. 249–254, Jun. 2002.
[53] E. Barzegaran, A. Joudaki, M. Jalili, A. O. Rossetti, R. S. Frackowiak, and M. G. Knyazeva, "Properties of functional brain networks correlate with frequency of psychogenic non-epileptic seizures," *Front Hum. Neurosci.*, vol. 6, p. 335, 2012.
[54] J. Kayser and C. E. Tenke, "Principal components analysis of Laplacian waveforms as a generic method for identifying ERP generator patterns: I. Evaluation with auditory oddball tasks," *Clin. Neurophysiol.*, vol. 117, no. 2, pp. 348–368, 2006.

Authors' photographs and biographies not available at the time of publication.